Contents lists available at ScienceDirect

Thin Solid Films

Structural and photoluminescence characterization of ZnO nanowalls grown by metal organic chemical vapor deposition

Jongsun Maeng, Gunho Jo, Minhyeok Choe, Woojin Park, Min-Ki Kwon, Seong-Ju Park, Takhee Lee *

Department of Materials Science and Engineering, Gwangju Institute of Science and Technology, Gwangju 500-712, Republic of Korea

A R T I C L E   I N F O

A B S T R A C T

We synthesized ZnO nanowall networks on GaN/sapphire substrates by metal organic chemical vapor deposition without using metal catalysts. It was observed that the domain size of ZnO nanowalls decreased and the density of nanowall networks increased with increasing growth time. The ZnO nanowall networks were grown in a crystallized wurtzite structure and c-axis growth direction perpendicular to the substrate. The temperature dependent PL spectra of ZnO nanowall networks grown for a short growth time show stronger emission of longitudinal optical first phonon replicas of free-exciton than free-exciton emission as temperature increases in ZnO nanowalls, compared with those grown for longer growth time. It is interpreted that different PL spectra of ZnO nanowall networks are due to different Ga impurity diffusion into ZnO on GaN epilayer.

1. Introduction

ZnO materials have attracted great interest for transparent electronic devices and optical devices such as thin-film transistors, light-emitting diodes, and laser diodes due to their unique properties, including a wide direct bandgap (~3.4 eV), large exciton binding energy (~60 meV), and piezoelectricity [1–3]. In particular, low dimensional ZnO nanostructures, such as one-dimensional (1-D) ZnO nanowires and zero-dimensional (0-D) ZnO quantum dots, have demonstrated enhanced device performance and potential applications such as nanoelectronic transistors and information-storage devices [4,5]. As compared with 1-D ZnO nanostructures, two-dimensional (2-D) ZnO nanostructures such as ZnO nanowalls have not been studied extensively. This may be because of the difficulty in controlling the shape of nanowalls due to the sensitivity to growth conditions [6]. ZnO nanowall networks can potentially be used for optoelectronics and sensors due to their large surface area, diverse shape, and ease of manipulation for device application [6–10]. In previous studies, it has been shown that 2-D ZnO nanowall networks can be synthesized in thermal evaporation based on the vapor–liquid–solid (VLS) growth method using metal catalysts or ZnO thin-film catalysts [7,8]. 2-D ZnO nanowall networks have also been synthesized by metal organic chemical vapor deposition (MOCVD) without using catalysts [6,9,10]. In particularly, the MOCVD technique has many advantages in terms of large area growth and accurate doping and thickness control [8]. Furthermore, in many cases, nanostructures grown without using metal catalysts are favored, since

metal catalysts may often act as defects of deep levels, resulting in degradation of device performance [11].

In this study, we synthesized the ZnO nanowall networks on a GaN/sapphire substrate without using metal catalysts. The surface morphology, structural characteristics, and photoluminescence (PL) properties of ZnO nanowall networks were investigated. We particularly compared the temperature dependent PL spectra of the nanowall networks grown for different growth times.

2. Experimental details

The schematic illustration in Fig. 1 shows the hot-wall MOCVD setup using diethylzinc [DEZn; $Zn(C_2H_5)_2$] and oxygen (O_2) gas as the Zn and O source materials for the growth of ZnO nanostructures, respectively. The DEZn bubbler was kept cool in a 10 °C temperature bath. Nitrogen as a carrier gas was passed through the DEZn bubbler, and DEZn precursors with nitrogen gas were supplied via inner quartz tube (5 mm diameter). Oxygen sources were supplied via outer quartz tube (30 mm diameter). In order to suppress generation of ZnO particles by pre-reaction between precursors and oxygen, DEZn and oxygen were supplied separately into the chamber and mixed over the substrate. DEZn and oxygen were typically supplied at flow rates of 5–20 μmol/min and 890 μmol/min, respectively. The ZnO nanostructures were synthesized on a GaN (2 μm thickness)/c-plane sapphire substrate without using metal catalysts at a growth temperature of ~800 °C. The chamber pressure was kept at 60 Torr for growing ZnO nanowall networks. The surface and cross-sectional images of ZnO nanostructures were observed by field emission scanning electron microscopy (FESEM). Structural analyses of synthesized ZnO nanostructures were carried out with X-ray diffraction spectroscopy (XRD) and high resolution transmission electron

* Corresponding author.
  E-mail address: tlee@gist.ac.kr (T. Lee).
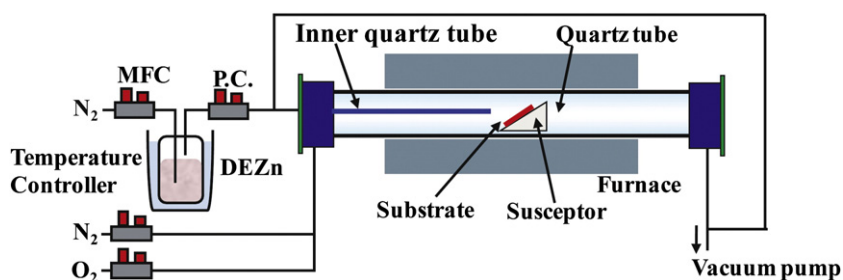
Fig. 1. Schematic illustration of hot-wall MOCVD system for synthesis of ZnO nanostructures.

microscopy (HRTEM). The PL spectra were measured from 10 to 300 K using a He–Cd laser of 325 nm wavelength as the excitation source.

3. Results and discussion

3.1. Morphological and structural analysis of ZnO nanowall networks

We investigated surface morphologies of ZnO nanowall networks grown for different growth times. Fig. 2 shows a series of the FESEM images of ZnO nanowall networks grown on the GaN/sapphire substrate at 800 °C for different growth time in the MOCVD system. Fig. 2(a) and (b), (c) and (d), and (e) and (f) shows sets of top-view and cross-sectional FESEM images of ZnO nanowall networks grown for 20, 30, and 60 min, respectively. We clearly observed that the surface morphology changed significantly with increasing growth time. The domain size of ZnO nanowalls decreased, and the density of nanowall networks increased with increasing growth time. The domain sizes of nanowalls were observed to be 100 nm–1.0 μm, 50–
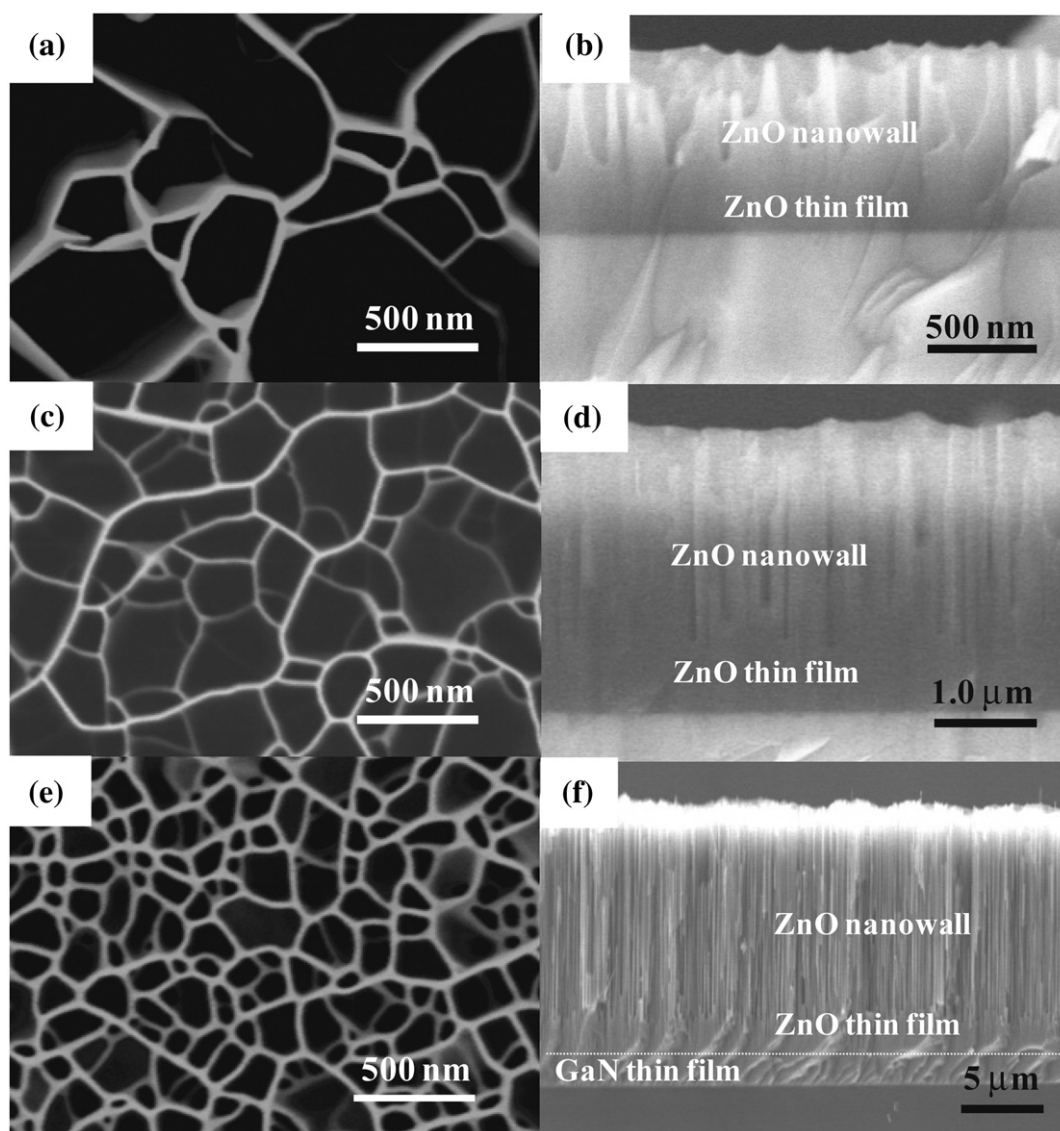
Fig. 2. FESEM images of ZnO nanowall networks grown on GaN/sapphire substrate at 800 °C under different growth times of (a and b) 20 min, (c and d) 30 min, and (e and f) 60 min. Images of (a), (c), and (e) are top views, and images of (b), (d), and (f) are cross-sectional views.

500 nm, and 30–300 nm for ZnO nanowall networks grown for 20, 30, and 60 min, respectively. The heights of nanowalls were found to be ~700 nm, ~2.5 μm, and ~10 μm for ZnO nanowall networks grown for 20, 30, and 60 min, respectively. The nanowall widths were found to be similar, 10–30 nm, for all of the ZnO nanowall networks. It should be noted that prior to growth of ZnO nanowall networks, a continuous ZnO thin film on the GaN/sapphire substrate of ~200 nm, ~600 nm, and ~2 μm thickness was grown for 20, 30, and 60 min, respectively. Note that ZnO nanowall thickness is not proportional to the deposition time, due to various reasons such as the different deposition rates of two ZnO structures (nanowall and thin film), preformation of ZnO thin films, and different domain sizes of ZnO nanowalls for different growth times.

The mechanism of forming ZnO nanostructures is commonly explained by vapor–liquid–solid (VLS) growth mechanism in which metal catalysts play an important role [2,7,8]. However, the ZnO nanowall networks grown in MOCVD method in our study do not follow the VLS mechanism because of the growth without using metal catalysts. It is known that ZnO growth along the [001] direction is favored, since the surface energy of the (001) plane is greater than that of the other crystal faces [12]. Kim et al. reported that when the Zn vapor flow was increased, the [001] direction crystallinity was improved; however, at the same time, the surface became more rough [10]. The ZnO nanowall networks can be formed with a sufficient supply of Zn adatoms. During the ZnO nucleation and growth stage, the high density ZnO nuclei on the substrate surface can be easily coalesced into [001] growth of ZnO nanostructures [8,10,13,14]. The continuous deposition of Zn vapor and oxidation results in forming the ZnO nanowall networks.

Fig. 3 shows XRD patterns and HRTEM images of ZnO nanowall networks to explain the detailed crystal information of ZnO nano-walls. The θ–2θ diffraction pattern of ZnO nanowalls in Fig. 3(a) indicates a good epitaxial relationship between the (001) plane of ZnO nanowalls and the GaN thin films epitaxially grown into c-axis direction on sapphire due to very intense (002) peaks and far weaker extra

(101) and (100) peaks. The (002) plane peaks of ZnO thin films and nanowalls, and GaN thin films are not resolved due to an excellent lattice matching between ZnO thin films and nanowalls and GaN thin films, as shown in Fig. 3(a) and (b). These results show that ZnO nanowalls are well crystallized and highly c-axis oriented. The full width at half maximum (FWHM) of the rocking curve of the (002) peak of ZnO nanowalls in Fig. 3(b) is 0.81°. This narrow FWHM of the rocking curve confirms that these nanowalls are well aligned and oriented along the [001] direction with their c-axis perpendicular to the substrate. The in-plane ϕ scan was performed by rotating the sample of grown ZnO nanowalls along the surface normal direction. Fig. 3(c) shows the ϕ scan at fixed 2θ angle 47.5° for the specific detection of (102) planes in ZnO nanowalls. The (102) plane family for ϕ scan analysis is chosen, since 2θ difference between ZnO (102) and GaN (102) is ~0.8°. The interference from each other could avoid due to enough 2θ difference and the individual spectra of ZnO nanowalls and GaN thin films could be obtained [15]. The six peaks were observed with an equivalent distance of 60°, indicating ZnO nanowalls on GaN epilayer with six-fold symmetry in the in-plane epitaxial relation. Fig. 3(d) shows the cross-sectional HRTEM image of ZnO nanowalls. The average atomic spacing along the growth direction was found to be ~0.26 nm. The lattice spacing of the (001) planes of wurtzite ZnO corresponds to ~0.52 nm, consistent with the lattice spacing observed from XRD patterns [14,16]. All results in Fig. 3 support the highly single crystallinity of ZnO nanowalls grown by MOCVD in this study.

3.2. Photoluminescence properties of ZnO nanowall networks

Fig. 4 displays the temperature dependent PL spectra measured from the top surface of ZnO nanowall networks. The PL spectra were measured for ZnO nanowall networks grown for 20, 30, and 60 min, as shown in Fig. 4(a), (b), and (c), respectively. PL measurement at low temperature and temperature evolution of PL peaks should be traced
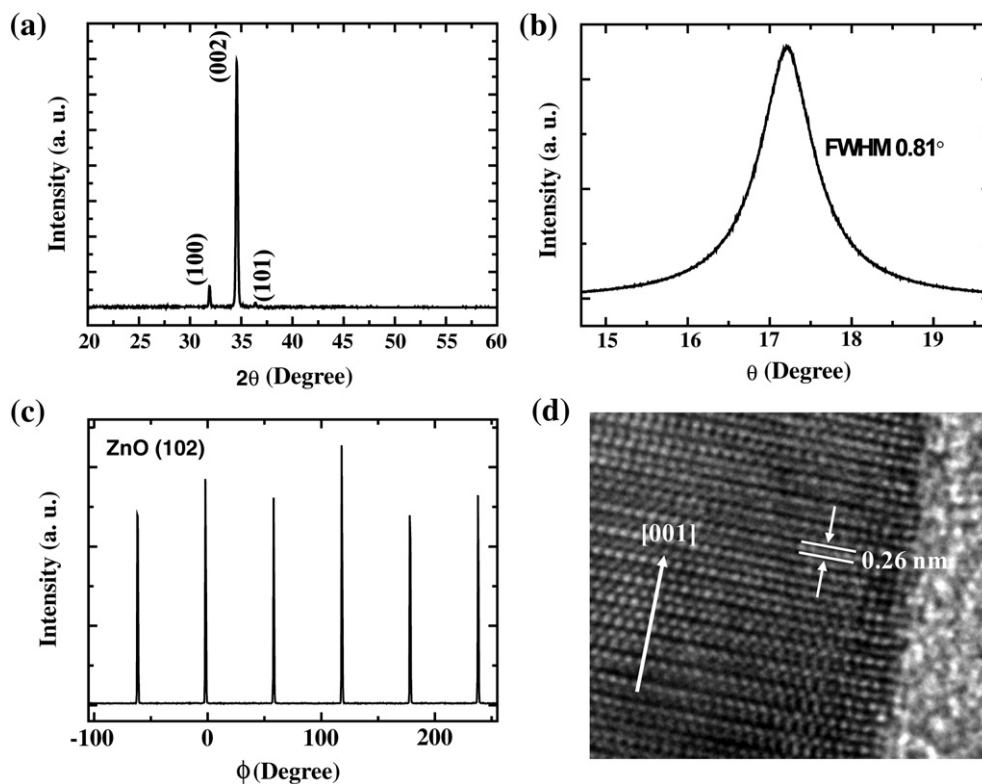
Fig. 3. XRD pattern and cross-sectional HRTEM image of ZnO nanowall networks grown for 30 min. (a) θ–2θ scan, (b) rocking curve, (c) ϕ scan of ZnO nanowall networks, and (d) cross-sectional HRTEM images of ZnO nanowalls.
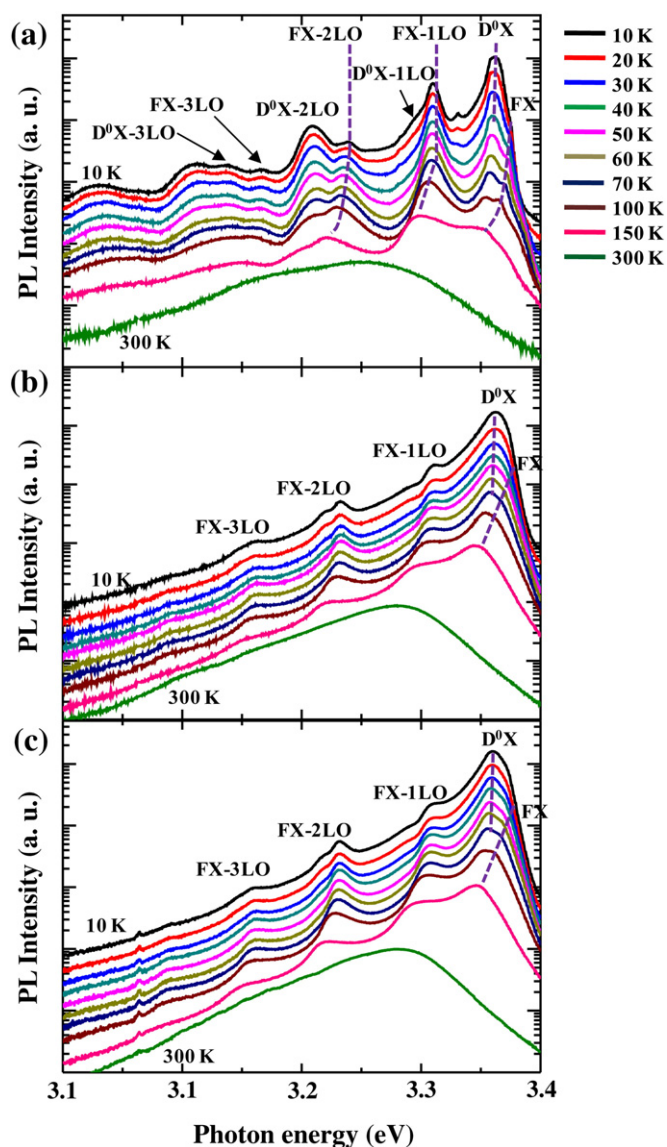
Fig. 4. PL spectra with logarithmic scale of ZnO nanowall networks grown for (a) 20 min, (b) 30 min, and (c) 60 min measured at various temperatures (10, 20, 30, 40, 50, 60, 70, 100, 150, and 300 K).

in order to confirm the corresponding assignments, since some of the PL peaks at room temperature are very weak or combined with closely narrow interval. The PL spectra at 10 K show excitonic behaviors associated with free-exciton (FX), longitudinal optical (LO)-phonon replicas of FX (FX-nLO), and LO-phonon replicas of donor-bound exciton (D^0X and D^0X-nLO). The emission peaks at 3.378, 3.360, 3.307, and 3.290 eV at 10 K are ascribed to FX, D^0X, FX-1LO, and D^0X-1LO. The bound exciton peak is generally related to the D^0X, since undoped ZnO is a native n-type semiconductor by oxygen vacancies which act as n-type dopants. The oscillatory structure of PL spectra with energy periodicity of ~70 meV was observed in LO-phonon replicas, which is ZnO characteristic electron–phonon interaction due to the ionicity of ZnO [17,18]. The emission peak locations at FX, D^0X, FX-nLO, and D^0X-nLO signals are consistent for ZnO nanowall networks grown for all growth times. On the other hand, the position of strong UV (ultraviolet) emission band at room temperature shifted from 3.25 eV to 3.28 eV with increasing growth time from Fig. 4(a) to (c). Additionally, the FWHM of UV emission PL peak measured at room temperature decreased from 140 meV to 90 meV with increasing growth time. At temperature below 100 K, the emission spectra of a D^0X peak are dominant. The intensity of the D^0X peak steadily be-

comes weaker, wider with the increase of temperature and eventually combined into the low energy shoulder of FX peak about 100 K. The D^0X related emissions were quenched due to thermal activation of the bound excitons and FX related emission became dominant as the temperature increases.

In particular, a stronger emission FX-1LO emission than FX emission was observed at higher temperature (>100 K) in ZnO nanowalls grown for 20 min (Fig. 4(a)), which have larger domain size and smaller height than those grown for the longer growth times of 30 and 60 min (Fig. 4 (b) and (c)). For the ZnO nanowall networks grown for 30 and 60 min, the FX emission was observed to be stronger than the FX-1LO emission for all measured temperatures. The FX-1LO emission observed in ZnO nanowall networks grown for 20 min can be associated with Ga incorporation into ZnO nanowalls on a GaN epilayer substrate. Schneider et al. reported that unintentional Ga incorporation into ZnO film from GaN substrate due to high growth temperature (777 ºC) led to bandgap narrowing along a cross-section of ZnO film from spatially resolved cathodoluminescence study [18]. Makino et al. explained PL band broadening at room temperature of Ga-doped ZnO by the contribution of LO-phonon replicas due to Ga impurities [20]. It is also known that the UV emission band of ZnO at room temperature suffered a red shift by Ga doping due to incorporation of shallow levels below the conduction band [20,21]. Therefore, strong FX-1LO emission (>100 K) and relative red shift of maximum UV emission at room temperature in PL spectrum of Fig. 4(a) are attributed to Ga incorporation into ZnO thin film. Ga from GaN layer can be diffused into the ZnO film (Fig. 2(a)) because ZnO film deposited prior to growth of nanowall networks has enough thin-film thickness (~200 nm) and sufficient growth times (20 min) to diffuse Ga from GaN, as expected in a previous study [19]. However, Ga incorporation into ZnO nanowalls would be negligible, since the ZnO nanowalls (height of ~700 nm) are grown above the ZnO thin film (~200 nm) and Ga cannot easily reach ZnO nanowalls by diffusing through the ZnO film.

The ZnO nanowalls and films with the Ga impurity diffused to different extents exhibit mixed PL properties of Ga-doped ZnO and undoped ZnO. The ZnO nanowall networks grown for 20 min, with the lowest thickness of ZnO thin film deposited prior to growth of nanowall networks among the three kinds of ZnO nanowall networks grown for three different growth times, are most significantly influenced by Ga incorporation. It is expected that Ga incorporation into ZnO thin films are more susceptible than that into ZnO nanowalls due to preformation of ZnO thin films and fast growth rate of ZnO nanowalls. Fig. 2(d) and (f) shows much thicker ZnO films and higher nanowalls than those of Fig. 2 (b). Due to the growth rate of ZnO nanowall networks being faster than the diffusion rate of Ga impurities expected from the previous study [19], ZnO nanowall networks grown for longer growth times exhibit less influence on PL properties due to Ga impurities. Therefore, the PL properties shown in Fig. 4(a) due to Ga incorporation into ZnO thin film are different from those shown in Fig. 4(b) and (c). Since the surfaces of ZnO nanowall networks grown for longer growth times have negligible Ga incorporation, these PL properties show stronger FX emission than FX-1LO emission without temperature dependence and display UV emissions into a higher energy range at room temperature. Significant variation in FX-phonon coupling is due to different annihilation process by lattice defects or related phonons at low temperature [20]. Different relative strength of FX-1LO to FX at low temperature emissions is due to the variations of concentration of impurities [20].

4. Conclusions

ZnO nanowall networks were synthesized on GaN/sapphire substrates by MOCVD method without using metal catalysts. Structural characterizations by XRD and HRTEM revealed that ZnO nanowall networks were single crystalline with c-axis growth direction. The temperature dependent PL spectra from ZnO nanowall networks grown for different growth times showed different excitonic and

phonon-assisted transitions. Strong FX-1LO emission (>100 K) and a red shift of maximum UV emission were observed in ZnO nanowall networks with the lowest thickness of ZnO thin film among the ZnO nanowall networks grown for three different growth times, which is due to being significantly influenced by Ga incorporation from the GaN epilayer. 2-dimensional ZnO nanowall networks can be a promising material structure for various electrical and optical applications due to the large surface area of nanowall networks.

Acknowledgments

References

[1] Ü. Özgür, Ya.I. Alivov, C. Liu, A. Teke, M.A. Reshchikov, S. Doğan, V. Avrutin, S.-J. Cho, H. Morkoç, J. Appl. Phys. 98 (2005) 041301.
[2] Z.L. Wang, J. Song, Science 312 (2006) 242.
[3] P.-K. Shin, Y. Aya, T. Ikegami, K. Ebihara, Thin Solid Films 516 (2008) 3767.
[4] W.I. Park, J.S. Kim, G.-C. Yi, M.H. Bae, H.-J. Lee, Appl. Phys. Lett. 85 (2004) 5052.
[5] J.H. Jung, J.Y. Jin, I. Lee, T.W. Kim, H.G. Roh, Y.-H. Kim, Appl. Phys. Lett. 88 (2006) 112107.
[6] Y.J. Hong, J. Yoo, Y.-J. Kim, C.-H. Lee, M. Kim, G.-C. Yi, Adv. Mater. 20 (2008) 1.
[7] H.T. Ng, J. Li, M.K. Smith, P. Nguyen, A. Cassell, J. Han, M. Meyyappan, Science. 300 (2003) 1249.
[8] S.-W. Kim, H.-K. Park, M.-S. Yi, N.-M. Park, J.-H. Park, S.-H. Kim, S.-L. Maeng, C.-J. Choi, S.-E. Moon, Appl. Phys. Lett. 90 (2007) 033107.
[9] C.-C. Wu, D.-S. Wuu, T.-N. Chen, T.-E. Yu, P.-R. Lin, R.-H. Horng, H.-Y. Lai, Jpn. J. Appl. Phys. 47 (2008) 746.
[10] S.-W. Kim, S. Fujita, M.S. Yi, D.H. Yoon, Appl. Phys. Lett. 88 (2006) 253114.
[11] W.I. Park, D.H. Kim, S.-W. Jung, G.-C. Yi, Appl. Phys. Lett. 80 (2002) 4232.
[12] W.I. Park, J. Yoo, G.-C. Yi, J. Korean Phys. Soc. 46 (2005) L1067.
[13] Z. Yin, N. Chen, R. Dai, L. Liu, X. Zhang, X. Wang, J. Wu, C. Chai, J. Crystal Growth 305 (2007) 296.
[14] C. Li, G. Fang, F. Su, G. Li, X. Wu, X. Zhao, Nanotechnology 17 (2006) 3740.
[15] Y.-K. Tseng, C.-T. Chia, C.-Y. Tsay, L.-J. Lin, H.-M. Cheng, C.-Y. Kwo, I.-C. Chen, J. Electrochem. Soc. 152 (2005) G95.
[16] J.Y. Lao, J.Y. Huang, D.Z. Wang, Z.F. Ren, D. Steeves, B. Kimball, W. Porter, Appl. Phys. A 78 (2004) 539.
[17] Y.-H. Cho, J.-Y. Kim, H.-S. Kwack, B.-J. Kwon, L.S. Dang, H.-J. Ko, T. Yao, Appl. Phys. Lett. 89 (2006) 201903.
[18] J. Grabowska, A. Meaney, K.K. Nanda, J.-P. Mosnier, M.O. Henry, J.-R. Duclère, E. McGlynn, Phys. Rev. B 71 (2005) 115439.
[19] R. Schneider, M. Schirra, A. Reiser, G.M. Prinz, W. Limmer, R. Sauer, K. Thonke, J. Biskupek, U. Kaiser, Appl. Phys. Lett. 92 (2008) 131905.
[20] T. Makino, Y. Segawa, S. Yoshida, A. Tsukazaki, A. Ohtomo, M. Kawasaki, H. Koinuma, J. Appl. Phys. 98 (2005) 093520.
[21] A. Escobedo-Morales, U. Pal, Appl. Phys. Lett. 93 (2008) 193120.